Dual hyperbolic-elliptic media

Carlos J. Zapata-Rodríguez,[a] David Pastor,[a] Pablo Cencillo,[a] Mario Avellaneda,[a]
Slobodan Vuković[b] and Juan J. Miret[c]

[a]Department of Optics, University of Valencia, Dr. Moliner 50, 46100 Burjassot, Spain;
[b]Center of Microelectronic Technologies and Single Crystals, Institute of Chemistry,
Technology and Metallurgy, University of Belgrade, Njegoševa 12, 11000 Belgrade, Serbia;
[c]Department of Optics, Pharmacology and Anatomy, University of Alicante,
P.O. Box 99, Alicante, Spain

ABSTRACT

Recent disclosures on subwavelength plasmonic crystals, like the potential excitation of a pair of coexisting wavefields with opposite refraction, only can be understood by considering two dispersion branches with completely different features that characterize the metamaterial. One branch gives elliptic-like dispersion and the other provides hyperbolic-like dispersion. However the effective medium approximation, also known as Rytov approximation, is not consistent with both curves simultaneously. We follow an approach leading to a single curve that allows a complete description of both diffraction behaviors concurrently. Importantly only two parameters of the closed curve, together with the lattice period, fulfill such a complete picture. In addition, our semi-analytical approach may include more general situations straightforwardly.

Keywords: optical properties, thin films, plasmonics

1. INTRODUCTION

Metal-dielectric superlattices are versatile metamaterials with unique dispersion properties. Recent advances in the fabrication of nanolayered devices have made possible to surpass the limit of the metal skin depth in the visible regime.[1] By means of resonant tunneling, alternate metal-dielectric strata become practically transparent. Furthermore, negative permittivity of metals demonstrates negative refraction for p-polarized waves.[2]

Modal coupling in adjacent nanomembranes gives rise to novel nonlocal effects. Recently it has been demonstrated that a single beam traveling in a homogeneous dielectric medium that impinges on a metallodielectric lattice is able to excite a couple of wavefields with opposite refraction.[3] This can be understood by considering independent dispersion curves for each beam diffracted in the metamaterial. However Rytov approximation,[4] later followed by Yeh,[5] is not consistent with both curves simultaneously.

In this contribution we follow an approach leading to a single elliptic curve that allows a complete description of both refractive behaviors concurrently. Importantly, only two parameters of the closed curve (the semi-axes of the resultant ellipse) together with the lattice period fulfill a complete picture for such an indefinite birefringence. For that purpose, wideness of the ellipse shall exceed that of the Brillouin zone. Additionally we analyze the inherent erroneous conduct of our approach in the vicinity of band edges. Finally our semi-analytical approach is extended to more general situations straightforwardly, including when a single plasmonic band comes into play.

2. DISPERSION IN PLANAR 1D SUBWAVELENGTH PLASMONIC CRYSTALS

The simplest metamaterial based on one-dimensional plasmonic crystals is that shown in Fig. 1. It consists of alternating planar strata of dielectric with positive dispersionless permittivity ϵ_d and metal with negative relative

Further author information: (Send correspondence to C.J.Z.-R.)
C.J.Z.-R.: E-mail: carlos.zapata@uv.es, Telephone: +34 963543805

Metamaterials VII, edited by Allan D. Boardman, Nigel P. Johnson, Richard W. Ziolkowski, Proc. of SPIE
Vol. 8423, 84231Z · © 2012 SPIE · CCC code: 0277-786X/12/$18 · doi: 10.1117/12.922118

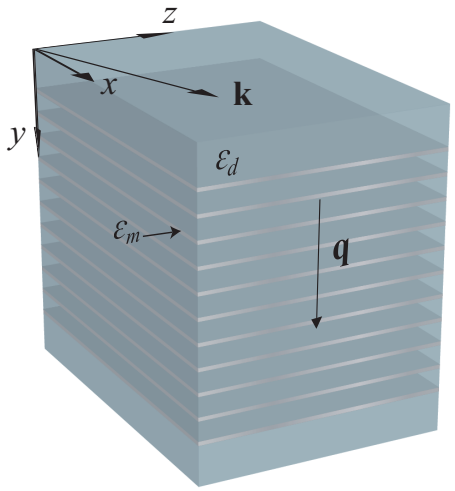

Figure 1. Geometry of the bilayer periodic structure; ϵ_m stands for permittivity in the metal, and ϵ_d for the dielectric.

dielectric constant ϵ_m in the frequency range of interest, that is visible and infrared frequencies. We use the simple Drude model for metal permittivity,

$$\epsilon_m(\omega) = 1 - \frac{\omega_p^2}{\omega^2}, \tag{1}$$

where ω_p is the plasma frequency of the metal. Fig. 1 depicts a periodic structure of bilayer unit cells as considered here for the subwavelength plasmonic crystal (SPC).

Let us write the thickness of a metal stratum as d_m, while the dielectric stratum thickness is d_d, making a total thickness of a bilayer unit cell of $L = d_m + d_d$. All of these values are constant throughout the multilayer. We assume that the thickness is much smaller than the operating wavelength, $L \ll \lambda$. For convenience, the spatial dimensions will be normalized to the metal skin depth, c/ω_p, and wavenumbers to $k_p = \omega_p/c$, where c is the speed of light in vacuum. Finally, we proceed by defining a synthetic parameter $\delta = d_m/L$, the filling factor of the multilayer, as the ratio of the metal stratum thickness to the total bilayer thickness.

Three-dimensional electromagnetic waves can propagate through the multilayer SPC structure shown in Fig. 1. The electromagnetic fields can be represented in the form

$$\mathbf{A} = \mathbf{u} A_q(y) \exp(iqy) \exp[i(k_x x + k_z z - \omega t)], \tag{2}$$

where $\mathbf{A}$ denotes either electric field $\mathbf{E}$, in the case of TE polarization, or magnetic induction $\mathbf{B}$, in the case of TM polarization. Therefore, Bloch wavevector $\mathbf{q} = q\mathbf{y}$ describes propagation perpendicular to the multilayer surface along the y-direction, and plasmonic wavevector $\mathbf{k} = (k_x, k_z)$ describes propagation along the metal-dielectric interfaces. In this case, the unitary vector $\mathbf{u} = (u_x, u_z)$ is orthogonal to $\mathbf{k}$.

For the case of an infinite multilayer one may write the well-known Floquet-Bloch dispersion relation, obtained as the eigenvalue solution for the transfer matrix,[6]

$$\cos(qL) = \cos(k_m d_m)\cos(k_d d_d) - \frac{1}{2}\left(\alpha_{s,p} + \frac{1}{\alpha_{s,p}}\right)\sin(k_m d_m)\sin(k_d d_d), \tag{3}$$

where

$$\alpha_s = k_m/k_d, \tag{4}$$

$$\alpha_p = k_m \epsilon_d / k_d \epsilon_m, \tag{5}$$

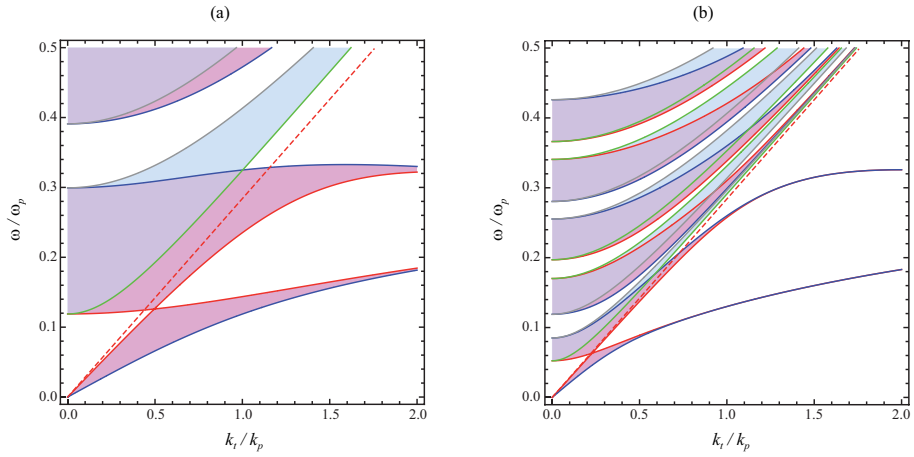

Figure 2. Dispersion of Ag-GaAs nanomembrane multilayer with $d_m = 0.5\ k_p^{-1}$ and two different values of d_d: (a) $d_d = 2.5\ k_p^{-1}$ and (b) $d_d = 10\ k_p^{-1}$. Dashed red line is the light line; areas in magenta represent allowed TM bands; zones in blue are allowed TE bands; solid red lines are TM band-edges crossing into the bandgap.

for the TE and TM polarization, respectively, and

$$k_{m,d} = \sqrt{k_0^2 \epsilon_{m,d} - k_t^2}. \tag{6}$$

Finally, $k_t = \sqrt{k_x^2 + k_z^2}$ denotes the transverse spatial frequency. Generally, when the right-hand side of Eq. (3) is lower than unity, we have allowed bands, while the opposite case defines the forbidden band (electromagnetic bandgap). Therefore, the band edges are defined by $\cos(qL) = \pm 1$. For subwavelength dimensions of the unit cell, there are two solutions for each sign, revealing four edge lines. Two of the edge lines may cross each other, depending on the value of filling factor δ as well as on the permittivity of the dielectric strata ϵ_d.

We performed exact calculations of the dispersion of planar SPCs for different widths d_d of the dielectric layers. Figure 2 shows the dispersion for a SPC made of Ag ($\omega_p = 12.9$ fs^{-1}) and GaAs ($\epsilon_d = 12.4$). In this configuration both TE and TM modes are supported. The metal filling factor was chosen within an interval ranging from $\delta = 0.048$ to $\delta = 0.167$. It can be seen that two TM allowed bands (magenta shaded areas) appear with a gap between them and two gaps outside (not shaded). The allowed bands are limited by band-edge lines. The inner band edges (red lines) are defined by the condition $\cos(qL) = +1$, while the two outer edges are determined by $\cos(qL) = -1$.

It is worth noting that zero group velocity (i.e. standing light) appears for both TE- and TM-polarized modes in the upper band for $k_t = 0$. Such slow states of light seem to correspond to Tamm plasmon polaritons.[7]

3. THE EFFECTIVE MEDIUM APPROXIMATION

When the SPC is infinite, and when the wavelength of the radiation is much longer than the size of the unit cell, it is usually assumed that the Rytov[4] or effective-medium approximation (EMA) is valid, and the metamaterial can be represented by a diagonal permittivity tensor $\bar{\epsilon} = \epsilon_\perp(\mathbf{xx} + \mathbf{zz}) + \epsilon_{||}\mathbf{yy}$, where

$$\epsilon_\perp = \frac{\epsilon_m d_m + \epsilon_d d_d}{L}, \tag{7}$$

$$\epsilon_{||} = \frac{\epsilon_m \epsilon_d L}{\epsilon_m d_d + \epsilon_d d_m}. \tag{8}$$

The indices $\perp$, $||$ indicate direction normal (x and z-directions) and parallel (y-direction) to the optical axes, respectively. Incidentally, implementation of metallic layers leads to positive birefringence, i.e. $\epsilon_{||} > \epsilon_\perp$, and in

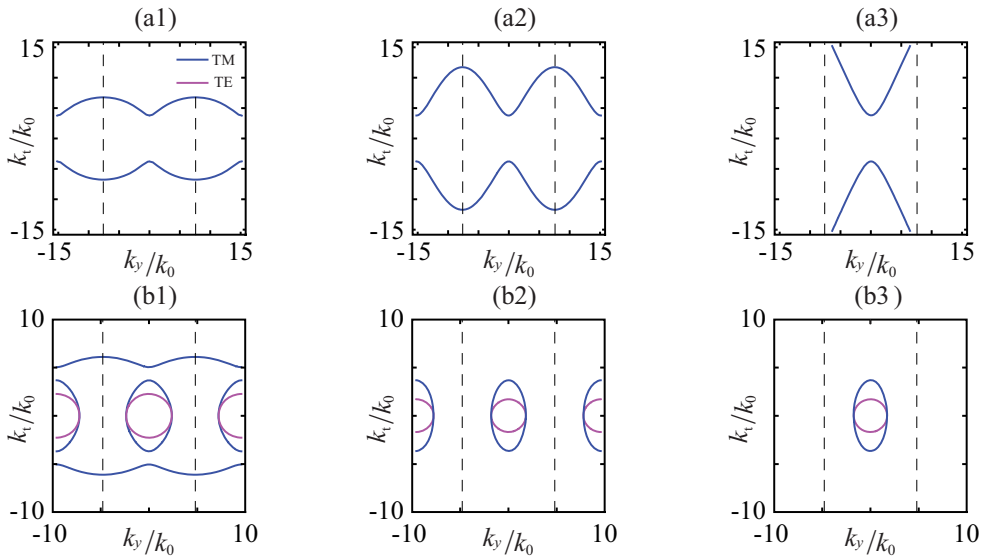

Figure 3. Equifrequency dispersion curves for an Ag-GaAs multilayer: $\lambda = 1.55\mu$m; $\epsilon_m = -116$; $\epsilon_d = 12.4$. In all cases $d_m = 12$nm. (1) Exact solutions; blue TM; magenta TE polarization; (2) QEMA approach; (3) conventional EMA theory; (a) $d_d = 90$nm; (b) $d_d = 150$nm.

dielectric-dielectric superlattices birefringence is always negative.[8] Then, general dispersion relation reduces to a pair of equations for the TE-polarized and TM-polarized modes,

$$k_x^2 + k_y^2 + k_z^2 = k_0^2 \epsilon_\perp, \tag{9}$$

$$\left(k_x^2 + k_z^2\right) \frac{\epsilon_\perp}{\epsilon_{||}} + k_y^2 = k_0^2 \epsilon_\perp. \tag{10}$$

Here, $k_0 = \omega/c = 2\pi/\lambda$ represents wavenumber in free space, while k_x, k_y, and k_z are the wavevector components in the (effective) media. Therefore k_y substitutes the pseudofrequency q used in Eq. (3). Since in the optical range of frequencies $\epsilon_m < 0$, and $\epsilon_d > 0$, it is clear that both $\epsilon_\perp$ and $\epsilon_{||}$ can change sign depending on layer thicknesses d_m and d_d. In the k-space, equation (9) represents a sphere, while equation (10) represents an ellipsoid, provided both $\epsilon_\perp$ and $\epsilon_{||}$ are positive. On the contrary, if $\epsilon_\perp/\epsilon_{||}$ is negative, Eq. (10) gives a hyperboloid of revolution.

Equations (9)-(10) are obtained from Eq. (3) by simple Taylor expansion by assuming $k_m d_m \ll 1$, $k_d d_d \ll 1$, as well as $qL \ll 1$. As can be easily seen, Eq. (3) is periodic in q, while Eqs. (9)-(10) for the EMA are not. To avoid this, k_y in (9)-(10) can be replaced by $(2/L)\sin(k_y L/2)$ to obtain quasi-effective medium approximation (QEMA).[7]

In order to get insight into validity of both EMA and QEMA theory we have solved numerically Eqs. (3), and compared the results with the corresponding approximations. We present some results in Fig. 3. As can be seen, EMA theory can be used in a limited range of parameters, and for a very limited range of k_t and k_y. QEMA is much better, but it does not reproduce the upper band in k_t for the TM-polarization. Besides the well known birefringence (circles for the TE- and ellipses for the TM-polarization), there exists the second TM-band. Thus, in a metal-dielectric superlattice, for sufficiently thin metallic layers, as well as for thin enough unit cells, we have two extraordinary TM-polarized modes (and one ordinary TE-polarized mode). One of these extraordinary p-polarized modes is represented by Eq. (10) using positive $\epsilon_\perp$ and $\epsilon_{||}$; also diffraction of the other mode could be approximated by the same equation (10) but using different permittivities provided they have a different sign. In this case we might speak of dual hyperbolic-elliptic media.

4. COMPLETE ELLIPTIC DISPERSION CURVE

A major problem in the description of the spatial dispersion curves for TM waves arises when the EMA provides positive values of $\epsilon_\perp$ and $\epsilon_{||}$ leading to an ellipsoidal curve; in this case the plasmonic band is completely missing.

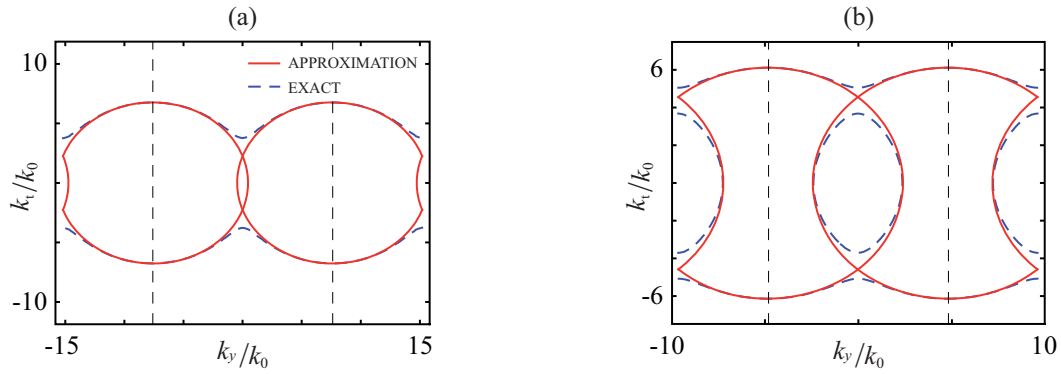

Figure 4. Equifrequency dispersion curves for an Ag-GaAs multilayer: $\lambda = 1.55\mu$m; $\epsilon_m = -116$; $\epsilon_d = 12.4$. In all cases $d_m = 12$nm. (a) $d_d = 90$nm and (b) $d_d = 150$nm. Exact solutions from Eq. (3) is drawn in dashed blue, and the approximation followed from Eq. (11) is in solid red.

In order to recover the high-frequency plasmonic band, we propose to use a simple curve-fitting method. Note that the maximum value of k_t associated with the plasmonic band is located at $k_y = (2m+1)\pi/L$, where m is an integer. Therefore we will include a set of data involving points from solutions of the exact dispersion equation (3) placed in the vicinity of the Brillouin boundaries. To find a formula that best fits this given set of data, for simplicity we propose a new ellipsoid of the form

$$\left(k_x^2 + k_z^2\right)\frac{\tilde{\epsilon}_\perp}{\tilde{\epsilon}_{||}} + \left[k_y - \frac{(2m+1)\pi}{L}\right]^2 = k_0^2\tilde{\epsilon}_\perp. \tag{11}$$

As a consequence, the maximum value of k_t is given by $k_0\sqrt{\tilde{\epsilon}_{||}}$.

For convenience, the data set is better fitted to the Taylor expansion of Eq. (11) around $k_y = (2m+1)\pi/L$. Up to a second order, we write $k_t = A - B\left[k_y - (2m+1)\pi/L\right]^2$, where $A = k_0\sqrt{\tilde{\epsilon}_{||}}$ and $B = (2k_0\tilde{\epsilon}_\perp)^{-1}\sqrt{\tilde{\epsilon}_{||}}$. Once we determine A and B from the parabolic-curve fitting, we may derive the semi-axes, $k_0\sqrt{\tilde{\epsilon}_{||}}$ and $k_0\sqrt{\tilde{\epsilon}_\perp}$, characterizing the off-center ellipsoids given in Eq. (11).

Figure 4 shows the dispersion curve for TM waves computed from the exact equation (3), for the two cases analyzed in Fig. 3. Also we include the ellipsoids derived from Eq. (11) after the corresponding curve fitting. We observe that the proposed ellipsoids provide accurate results except in the vicinities of $k_y = 0$ (more generally around $k_y = 2m\pi/L$). In this region, two neighboring ellipsoids cut at a certain value of k_t, what happens merely if $\sqrt{\tilde{\epsilon}_\perp} > \pi/k_0L$. From physical fundamentals we expect that, in this case, Bragg reflections comes into action and consequently bandgaps emerge. Note that Eq. (11) itself does not provide an accurate spatial dispertion near the bandgaps but it reveals its presence in a simple way.

In the case that two TM bands are present, it is espected that the value of $k_0\sqrt{\tilde{\epsilon}_\perp}$ were higher than π/L, as we have mentioned above. In fact we estimate that $k_0\sqrt{\tilde{\epsilon}_\perp} = k_0\sqrt{\epsilon_\perp} + \pi/L$, that is an accurate equation provided $\epsilon_\perp \geq 0$. This equation may be rewritten as

$$\tilde{\epsilon}_\perp = \left(\sqrt{\epsilon_\perp} + \frac{\pi}{k_0L}\right)^2. \tag{12}$$

This is a relevant result since it can be used to estimate analytically the value of $\tilde{\epsilon}_\perp$ instead of employing the proposed curve fitting.

In Fig. 5(a) we represent the values of $\tilde{\epsilon}_{||}$ and $\tilde{\epsilon}_\perp$ that are calculated by the method based on the curve fitting described above. Those estimates are depicted together with $\epsilon_{||}$ and $\epsilon_\perp$ provided by Eqs. (7) and (8) from the EMA, shown in Fig. 5(b). We observe that $\tilde{\epsilon}_{||}$ and $\tilde{\epsilon}_\perp$ are always positive parameters. However, $\epsilon_{||}$ and $\epsilon_\perp$ may change of sign; in the Figure 5(b) we show a case where only $\epsilon_\perp$ takes either a positive or a negative value. We

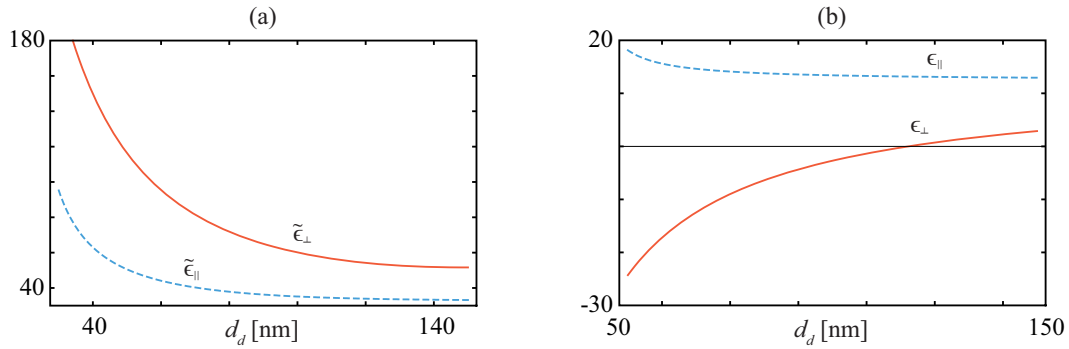

Figure 5. (a) Estimations of $\tilde{\epsilon}_{||}$ and $\tilde{\epsilon}_\perp$ from the curve-fitting method for an Ag-GaAs multilayer at $\lambda = 1.55\mu$m. Again $d_m = 12$nm in all cases. (b) Average permittivities predicted by the EMA and calculated from Eqs. (7) and (8).

point out that some plasmonics metamaterials are of the form such that the EMA estimates an hyperboloidal dispersion, specifically when $\epsilon_\perp/\epsilon_{||} < 0$, in opposition of the ellipsoidal dispersion given by our approach, since $\tilde{\epsilon}_{||} > 0$ and $\tilde{\epsilon}_\perp > 0$.

5. CONCLUSIONS

We analyzed 3D electromagnetic wave propagation along planar metal-dielectric multilayers, which represent the simplest subwavelength plasmonic crystals. The dispersion of plasmon wavevectors for various multilayer geometries is investigated following different approaches. In particular, Rytov's model of effective medium is unable to reproduce multiband dispersion associated with TM modes in the great majority of circumstances. For two-fold bands, one branch of these extraordinary p-polarized modes is represented by using positive $\epsilon_\perp$ and $\epsilon_{||}$, and the other branch is approached similarly but using different permittivities provided they have an opposite sign; here this is referred to dual hyperbolic-elliptic media. However the EMA provides the first branch exclusively. Differently we propose a simple, single equation that, in this aspect, improves the results derived from the EMA. Spatial dispersion is formulated in terms of a set of off-center ellipsoids, which semi-axes are given by $k_0\sqrt{\tilde{\epsilon}_{||}}$ and $k_0\sqrt{\tilde{\epsilon}_\perp}$. Specifically some plasmonics metamaterials are of the form such that the EMA estimates an hyperboloidal dispersion in opposition of the ellipsoidal dispersion given by our approach.

ACKNOWLEDGMENTS

This research was funded by the Spanish Ministry of Economy and Competitiveness under the project TEC2009-11635, by the Qatar National Research Fund under the project NPRP 09-462-1-074, and by the Serbian Ministry of Education and Science under the projects III 45016 and TR 32008.

REFERENCES

1. P. Chaturvedi, W. Wu, V. J. Logeeswaran, Z. Yu, M. S. Islam, S. Y. Wang, R. S. Williams, and N. X. Fang, "A smooth optical superlens," *Appl. Phys. Lett.* **96**, p. 043102, 2010.
2. M. Scalora, G. D'Aguanno, N. Mattiucci, M. J. Bloemer, D. de Ceglia, M. Centini, A. Mandatori, C. Sibilia, N. Akozbek, M. G. Cappeddu, M. Fowler, and J. W. Haus, "Negative refraction and sub-wavelength focusing in the visible range using transparent metallo-dielectric stacks," *Opt. Express* **15**, pp. 508–523, 2007.
3. A. A. Orlov, P. M. Voroshilov, P. A. Belov, and Y. S. Kivshar, "Engineered optical nonlocality in nanostructured metamaterials," *Phys. Rev. B* **84**, p. 045424, 2011.
4. S. M. Rytov, "Electromagnetic properties of layered media," *Sov. Phys. JETP* **2**, p. 466, 1956.
5. A. Yariv and P. Yeh, "Electromagnetic propagation in periodic stratified media. II. birefringence, phase matching, and x-ray lasers," *J. Opt. Soc. Am.* **67**, pp. 438–448, 1977.
6. P. Yeh, *Optical Waves in Layered Media*, Wiley, New York, 1988.

7. S. M. Vukovic, I. V. Shadrivov, and Y. S. Kivshar, "Surface Bloch waves in metamaterial and metal-dielectric superlattices," *Appl. Phys. Lett* **95**, p. 041902, 2009.
8. D. Artigas and L. Torner, "Dyakonov surface waves in photonic metamaterials," *Phys. Rev. Lett.* **94**, p. 013901, 2005.